

NEW TEST APPROACH AND EVALUATION OF DYNAMIC AND THERMAL PARAMETERS OF ELASTOMERS

Luděk Pešek, František Vaněk, Pavel Procházka, Vítězslav Bula, Jan Cibulka*

The new test approach for evaluation of thermo-visco-elastic parameters of elastomers is designed, realized and discussed herein. The main attention is devoted to a kinematically excited rubber beam specimen under transient resonant sweep excitation. Mechanical material characteristics, i.e. Young modulus and loss angle, are identified from analytical formulas of frequency response function based on measured dynamic loading and response signals. Heat material constants were estimated indirectly by numerical thermo-mechanical FE model and matching numerical and experimental results. The 'sweep' regime tests serve for estimation of thermal and mechanical dependences. Long-term fatigue tests with cyclic resonant loading enable analysis of material degradation, such as hardening and permanent deformations.

Keywords: rubber, dynamic, tests, identification, fatigue, thermo-mechanics

1. Introduction

The rubberlike materials in contradiction to classical construction materials undergo much stronger time dependent behavior during dynamic loading caused by processes as creep, crystallization and aging. Furthermore the material behavior is very temperature dependent. Some changes are reversible and the materials recover but some of them are irreversible and cumulate according to the history of mechanical and thermal loadings [1, 2].

Synthetic rubbers with higher hardness in a range Sh 70–80 have been tested on the expensive hydraulic machines with a costly operation in the Institute [3]. The cost of operation is mainly remarkable at low frequency loading and high number of cycles 10^7 – 10^8 required for the fatigue tests. Therefore for speeding up the fatigue tests the resonance pulsators under pressure-tension stress are used that can operate in resonance with a lower energy consumption and higher frequency of loading. Higher frequency, however, can lead to heating of the specimens due to high dissipation of mechanical energy by inner damping. Therefore we search new methods of elastomer testing that could be performed in laboratory conditions and with common measurement and loading tools.

In this paper the experimental method for determination of dynamic and thermal parameters of elastomers, i.e. dynamic stiffness, damping, thermal capacity and thermal conductivity, is proposed by means of a mathematical model of the specimen. These parameters are evaluated from flexural vibrations of cantilever beam at a kinematic excitation. The kinematic excitation is profitably used for lifetime tests of metallic structures and therefore this excitation is also proposed for elastomers with extension to dynamic response measurements and identifications of their material parameters. The accurate parameter identification can

* Ing. L. Pešek, CSc., Ing. F. Vaněk, CSc., Ing. P. Procházka, CSc., Ing. V. Bula, J. Cibulka, Institute of Thermomechanics AS CR, v.v.i., Dolejškova 5; 182 00 Praha 8

serve for evaluation of material changes on temperature and loading history. The fatigue long-term test was conducted under regime of a stationary first resonance beam vibration and at scheduled test interruptions the eigenvalues of the beam are identified for Young modulus and loss angle evolutions. The eigenvalues are identified by a fitting algorithm from complex frequency response functions (FRF) that are determined from beam vibrations excited by low rate frequency swept loadings over the first resonance vibration.

As the next parameter of the material change the permanent deformation is evaluated, too. This deformation is computed from a drop of the free end of the beam. During the dynamic test temperature is measured on the beam surface at the place of maximum beam heating and the temperature parameters are estimated based on thermo-mechanic numerical model.

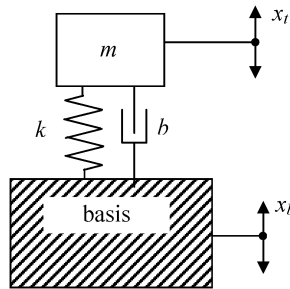


Fig.1: Kinematic excitation of a Kelvin-Voigt supported mass

2. Frequency response function for kinematic excited clamped beam

The excited basis connected with the rubber beam described by a stiffness k , a mass m and a damping b can be schematically depicted as a model of kinematic excited Kelvin-Voigt supported mass (Fig. 1). The total movement of the mass m consists of a basis displacement x_b and relative movement x_r of the mass that is linked with the basis via the viscous-elastic support. Hence

$$x_t = x_r + x_b . \quad (1)$$

When the finite element method is used for numerical modeling of flexural beam vibration the mass, stiffness and damping become matrices \mathbf{M} , \mathbf{K} and \mathbf{B} . Then displacements x_r , x_t , velocities \dot{x}_r , \dot{x}_t and accelerations \ddot{x}_r , \ddot{x}_t of the supported mass become corresponding vectors designated by capital letters whose components are related to the beam nodal movements describing the motion of the FE model. The equation of motion for kinematic excited beam can be expressed

$$\mathbf{M} \ddot{\mathbf{X}}_t + \mathbf{B} \dot{\mathbf{X}}_r + \mathbf{K} \mathbf{X}_r = \mathbf{0} \quad (2)$$

and after substituting the Eq. (1) we receive

$$\mathbf{M} \ddot{\mathbf{X}}_r + \mathbf{B} \dot{\mathbf{X}}_r + \mathbf{K} \mathbf{X}_r = -\mathbf{M} \mathbf{I} \ddot{x}_b, \quad (3)$$

where \mathbf{I} is a zeros vector with units on positions corresponding to the kinematic inertia forces proportional to the scalar function \ddot{x}_b describing acceleration of the basis.

So, the exciting force of the beam is defined as inertia force of the beam mass from the basis acceleration. In the frequency domain the difference of total and relative motions in

arbitrary j^{th} node of the beam can give the harmonic movement of the basis in the following way

$$\ddot{y}_b = \ddot{y}_{tj} - \ddot{y}_{rj} , \quad \dot{y}_b = \dot{y}_{tj} - \dot{y}_{rj} , \quad y_b = y_{tj} - y_{rj} , \quad (4)$$

where the relative motion \ddot{y}_{rj} , \dot{y}_{rj} , y_{rj} is defined by the frequency response function (FRF) H_j between the kinematic inertial excitation uniformly distributed along a beam length and a response in the j^{th} node :

$$\begin{aligned} y_{rj}(\omega) &= H_j(\omega) \ddot{y}_b(\omega) = \omega^2 H_j(\omega) y_b(\omega) , \\ \dot{y}_{rj}(\omega) &= \omega H_j(\omega) \dot{y}_b(\omega) = \omega^2 H_j(\omega) \dot{y}_b(\omega) , \\ \ddot{y}_{rj}(\omega) &= \omega^2 H_j(\omega) \ddot{y}_b(\omega) . \end{aligned} \quad (5)$$

The FRF for non-conservative self-adjoin mechanical system given by the Eq. 3 is defined [4] as

$$H_j = \sum_{\nu} \frac{x_{\nu j} (\mathbf{X}_{\nu}^T \mathbf{M} \mathbf{I})}{i\omega - \mathbf{s}_{\nu}} + \sum_{\nu} \frac{\bar{x}_{\nu j} (\bar{\mathbf{X}}_{\nu}^T \mathbf{M} \mathbf{I})}{i\omega - \bar{\mathbf{s}}_{\nu}} , \quad (6)$$

where \mathbf{s}_{ν} , \mathbf{X}_{ν} are the ν^{th} eigenvalue and the corresponding right-side orthonormal eigenvector, respectively. The term $x_{\nu j}$ is the j^{th} component of the eigenvector \mathbf{X}_{ν} . The line over the letter denotes a complex conjugate counterpart.

For computation of \ddot{y}_b , \dot{y}_b , y_b the Eq. 5 will be substituted into the Eq. 4

$$\ddot{y}_b = \ddot{y}_{tj} - \omega^2 H_j \ddot{y}_b , \quad \dot{y}_b = \dot{y}_{tj} - \omega^2 H_j \dot{y}_b , \quad y_b = y_{tj} - \omega^2 H_j y_b . \quad (7)$$

Then using the Eq. 7 and Eq. 4 we can get the FRF function H_j either by means of total \ddot{y}_{tj} or relative y_{rj} response of the beam

$$H_j = \frac{\ddot{y}_{tj} - 1}{\omega^2 \ddot{y}_b} = \frac{y_{rj}}{\ddot{y}_b} . \quad (8)$$

For verification of the (6) and (8) the FRF evaluated according to this relation using eigenvalues and eigenvectors of the numerical beam model was compared with the FRF directly calculated by harmonic analysis of the 3D beam model. The cantilever beam was kinematical excited in the program ANSYS. The amplitude-frequency characteristic of analytical accelerance function $\omega^2 H_j$ computed both by the (6) (solid line) and by (8) namely $(y_{tj}/y_b - 1)$ (dashed line) by harmonic analysis for unit basis amplitude y_b at the free end of the beam are depicted in Fig. 2.

Dimensions and material parameters of the numerical beam model were: a width $a = 40$ mm, a height $b = 16$ mm, a length $l = 200$ mm, a density $\rho = 1.5 \times 10^3$ kg/m³, Young modulus $E_{\text{DYN}} = 55$ MPa, damping ration $\xi_1 = 0.08$, stiffness coefficient of proportional damping $\beta_K = 2 \times 10^{-3}$, the computed first flexural eigenfrequency $f_1 = 12.8$ Hz.

3. Experimental procedure

For evaluation of dynamic elastomer behavior such as dynamic Young modulus and loss factor the short-term tests of the cantilever beam under sweep kinematic excitation with a lower speed rate running over the first flexural eigen-resonance were used. The

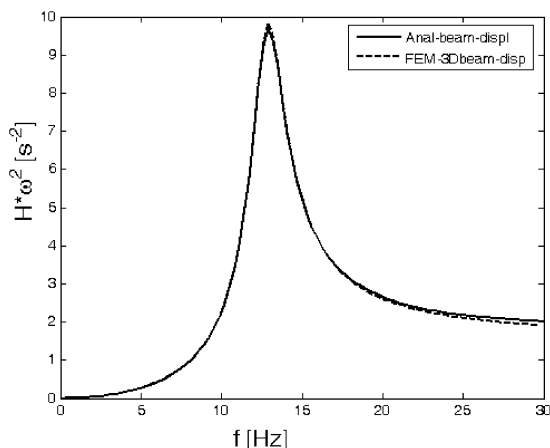


Fig.2: Comparison of analytical and FEM computations of amplitude-frequency acceleration function

dynamic behavior is derived from the dynamic beam characteristic, i.e. eigen-frequency and damping ratio, that were identified from FRFs of measured basis acceleration \ddot{x}_b moving the beam versus selected beam point total and/or relative responses \ddot{x}_{tj} , x_{rj} , respectively. The acceleration \ddot{x}_{tj} was measured on the end of the beam and the relative end beam displacement x_{rj} was derived from the strain-gauge measurement.

The scheme of the rubber beam clamping and beam dimensions are in Fig. 3. Preliminary rubber constants are: a density $\rho = 1.477 \times 10^3 \text{ kg/m}^3$, dynamic Young modulus $E_{\text{Dyn}} = (55\text{--}60) \text{ MPa}$, static Young modulus $E_{\text{Stat}} = 32 \text{ MPa}$, damping ratio $\xi_1 = (0.055\text{--}0.075)$.

The powerful electrodynamic vibrator B&K 4018 (dynamic force up to 1780 N, static force max. 445 N, maximal mass of a test body 2 kg, frequency range up to 4.5 kHz) realized excitation of basis. The vibrator was controlled either by the numerical program written in Data acquisition toolbox (DAQ) of MATLAB programming environment for the case of sweep sine loading or by an accurate generator for the case of cyclic resonance fatigue tests. The A/D converter NI PCI-6035E and the program in DAQ provided a digitalization of measured analog signals that were further processed by developed programs in Matlab2007b.

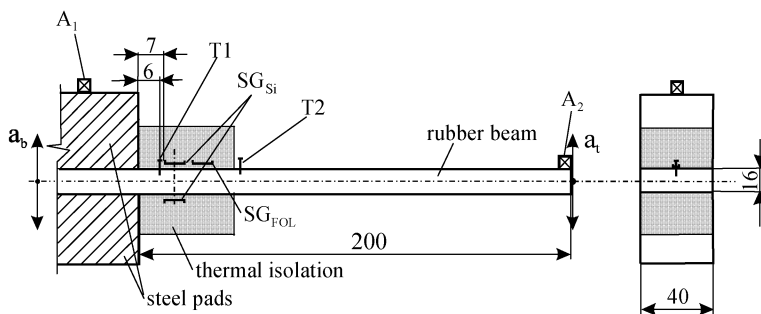


Fig.3: Sketch of cantilever rubber beam and placements of sensors

Vibration of the rubber beam was measured by four sensors: a) and b) feedback capacity accelerometers Motorola MMA6231Q of dimensions $5 \times 5 \times 3 \text{ mm}$ and range $\pm 10 \text{ g}$ placed on the basis (A_1 – acceleration a_b) and on the free beam end (A_2 – acceleration a_t), respectively,

c) silicon strain-gauge SG_{Si} (strain ε_1) and d) foil strain-gauge SG_{FOL} (ε_2) placed on the longitudinal axis at the vicinity of the clamping. Two silicon strain-gauges VTS – ZLÍN AP145-5-100 connected into strain-gauge semi-bridge (max. strain 0.35 %) were cemented at the clamping – one on the upper and the other on the bottom side of the beam. The foil strain-gauge HBM 1-LD20-10-120 that enables to measure strains up to 10 % with the cycle limit 10^7 was placed on the upper side of the beam, too. Contrary to the foil strain-gauges the silicon ones have 140 higher sensitivity.

Since the beam end drop during fatigue tests was selected for determination of the permanent deformation of rubber, the change of beam free end position and the change of basis table position with respect to the stator part of vibrator were recorded and used for evaluation of the drop.

For measurement of relative table position was used the Eddy current displacement sensor SCHENCK 0801 and for relative end beam position was measured by optical PSD photodetector PCD6004A. A line laser OLP-503PL was used as a light source. The size of trace on PSD detector proportionally changed by shading the falling light with moving end of the beam and by that the signal of the detector proportionally changed.

For detection of fast and small temperature changes in orders of hundredth degrees of Celsius platinum temperature sensors M-FK622 (size $6 \times 2.2 \times 0.9$ mm) was manufactured by thin layer technology of platinum sputtering on the corundum pad HERAEUS Sensors. Thanks to a high basic electrical resistance $2 \text{ k}\Omega$ very small measuring current $100 \mu\text{A}$ flows through the sensor and causes very small heating. This thin layer technology using the thermal non-conductive pad enables to measure temperature with short response 0.7 s for rubber materials. Two these sensors were placed on the beam. One was at the beam clamping (T1) and the other (T2), a reference, were 50 mm aside from the clamping. The reference sensor served for evaluation of temperature increment under the dynamic loading.

a) Swept excitation

Frequency characteristics of rubber beam were ascertain from measurement of vibrator table motion and dynamic responses of the beam under bi-directional swept frequency excitation with a rate 0.2 Hz/s and 0.4 Hz/s in a range from 3 Hz to 28 Hz.

Since the behavior of rubber materials is non-linear with respect to a vibration amplitude the frequency characteristics were evaluated for different levels of excitation amplitudes. The gain of the powerful amplifier was set from 1 to 4 what covered a range of vibrator table amplitudes from 2×10^{-4} m to 7×10^{-4} m in the first flexural resonance.

Measured analog signals of accelerations and strains were digitalized with sampling frequency 10 kHz and then low-pass filtered by the cut-off frequency 100 Hz. The ‘cleansed’ signals of accelerations a_b and a_t are depicted in the Fig. 4. The maxima and their corresponding times (Fig. 5a,b) for each vibration period are searched by the mapping algorithm. These values are used for a computation of amplitudes, phases and excitation frequencies of FRFs (Fig. 5c,d). Since the excitation frequency is changeable during sweep loading a frequency step of the evaluated FRF is not equal. Therefore before the classical identification by the method of curve fitting LSFD [5] the FRFs were interpolated to obtain an equidistant frequency step. All numerical algorithms used for the signal processing, i.e. filtering, mapping, interpolation and identification, were programmed in MATLAB2007 utilizing the toolbox Signal Processing.

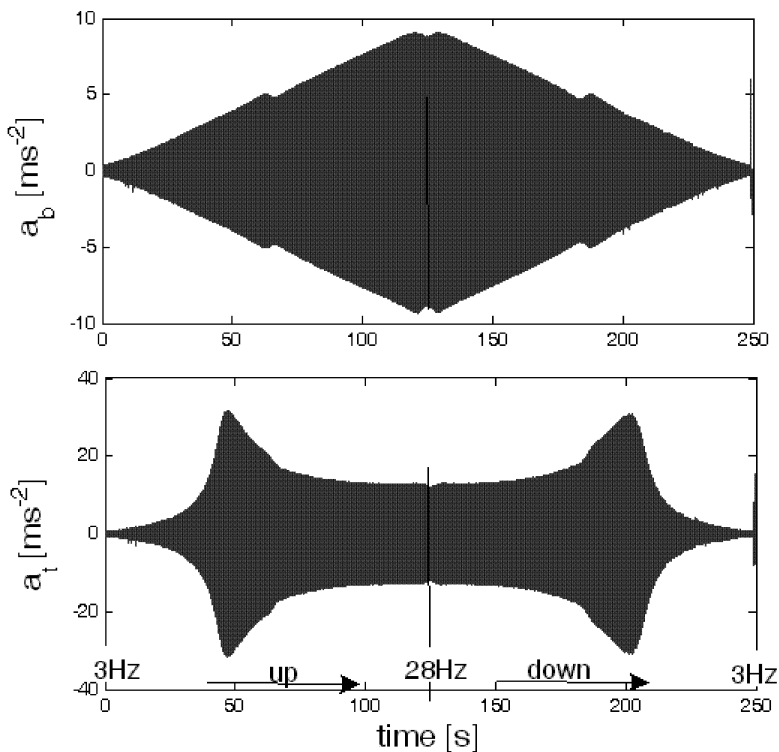


Fig.4: Time characteristics of basis acceleration a_b and free beam end acceleration a_t

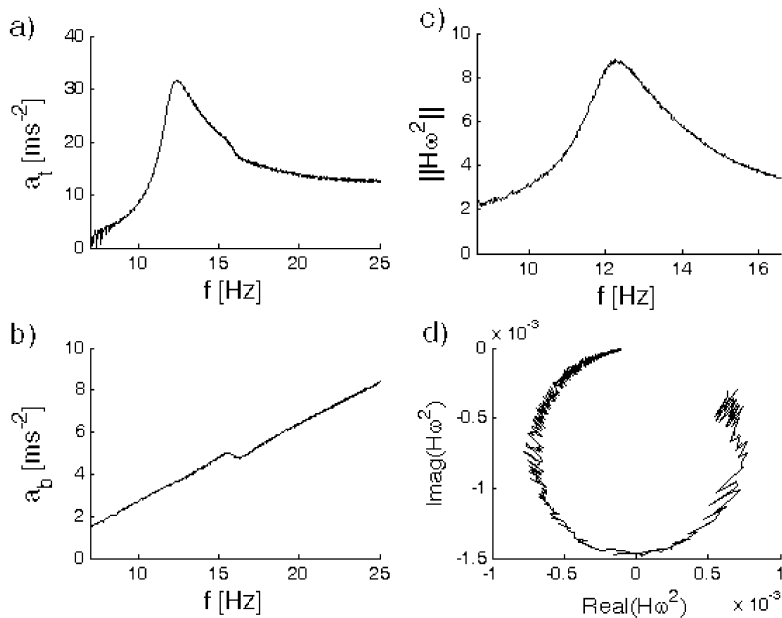


Fig.5: Characteristics of beam-end maxima (a) and basis maxima (b), amplitudo-frequency function of accelerance (c) and Nyquist diagram of accelerance (d)

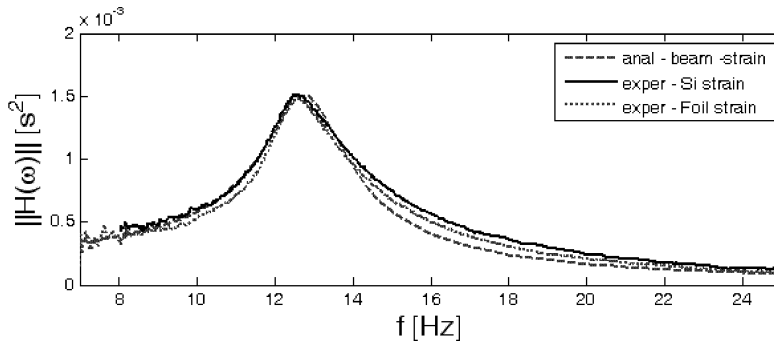


Fig.6: Comparison of FRF functions: analytical approach, experimental evaluation – silicon and foil strain-gauge measurements

The comparison between analytical calculation of FRF (Eq. 6) and experimental evaluation using a ratio between strain-gauge response and vibrator table acceleration maxima (Eq. 8) is shown in the Fig. 6. For analytical calculation the 1D model of beam elements with the same numerical parameters was used as for the harmonic analysis of 3D beam model. Since the beam model was considered as undamped the non-complex real eigenvectors \mathbf{Y}_ν were mass-orthonormalized and according to [6] the eigenvectors of the nonconservative system were approximated by

$$\mathbf{X}_\nu = \frac{\mathbf{Y}_\nu}{\sqrt{2i\omega_\nu}},$$

where ω_ν is ν -natural frequency of the undamped model and i is an imaginary unit.

b) Cyclic excitation

Cyclic excitation of fatigue tests changed in a range 11.8 Hz up to 12.8 Hz according to actual first flexural beam resonance. The level of the table vibration was 7×10^{-4} m. The loading blocks lasted from 8 to 10 hours during day hours. Total loading time was about 149 hours. The rubber beam was not tempered and the test was performed at a surrounding room temperature.

At the end of the time blocks the mean values and amplitudes were recorded on all sensors. Furthermore the drop of the free end of the beam was observed for the permanent deformation evaluation. After finishing the fatigue excitation the beam was loaded by the sweep excitation and the identified results were compared with original state.

The characteristics of identified eigenfrequencies (Fig. 7) of the rubber beam show that the strain-gauge and accelerometer measurements give practically the same results. The differences are in a range of measurement uncertainty. Furthermore the damping increases and the frequency decreases with an increase of the table vibration level what describes the non-linear behavior of the rubber material. The next finding is that the eigenfrequencies increased by 0.5 Hz after the fatigue test. It corresponds to stiffening the rubber. A range of strains was from 0.1% up to 0.2% (maximum level of the excitation). From numerical modeling the eigenfrequency f_1 can be recalculated to Young modulus by means of Bernoulli-Euler beam theory

$$E_{\text{DYN}} = 38.3 \frac{\varrho l^4}{b^2} f_1^2, \quad (9)$$

where ϱ is rubber density, l a beam length, b a beam thickness. For our dimensions of beam

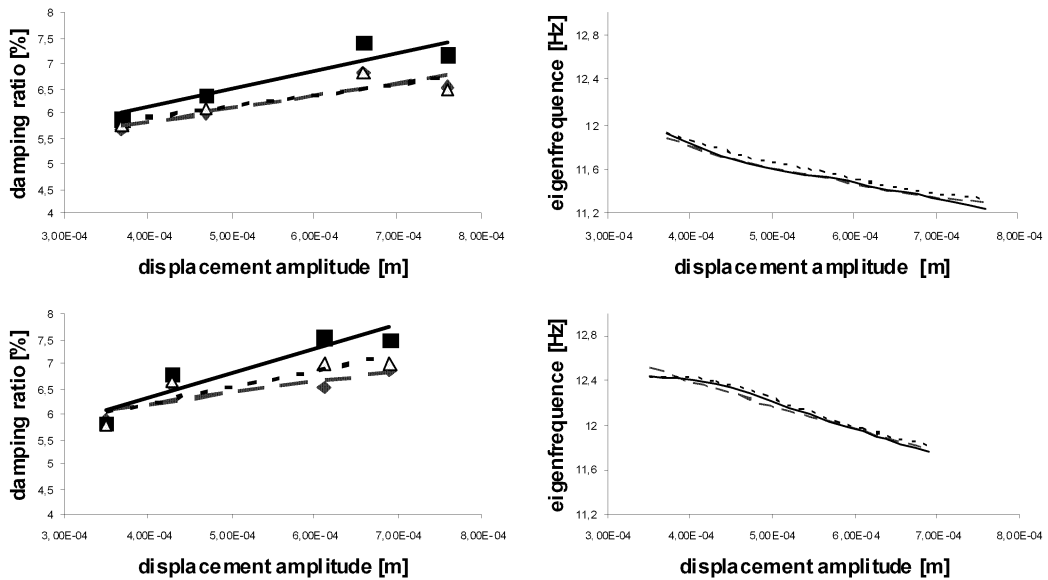


Fig.7: Evaluations of eigenfrequency f_1 and damping ratio $\xi_1 \times 100$ [%] at the beginning (top) and the end (bottom) of strain-gauge and accelerometer fatigue measurements – Si strain-gauge (solid), foil strain gauge (dotted), accelerometer (dashed line)

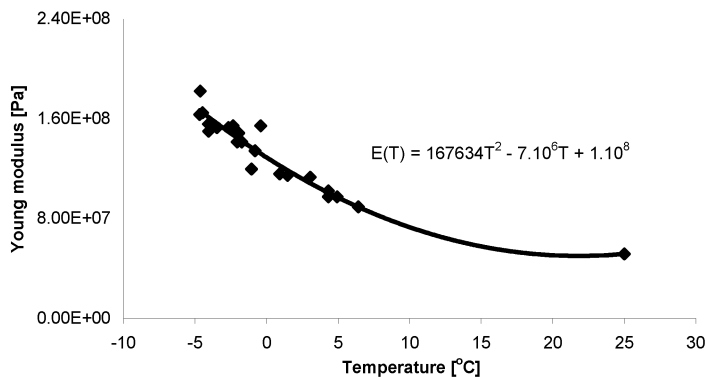


Fig.8: Young modulus versus temperature characteristic

and the measured frequency $f_1 = 12.5\text{Hz}$ we get $E_{\text{DYN}} = 55.2\text{MPa}$. Loss angle δ can be obtained from a damping ratio by an expression $\delta = \arctan(2\xi)$ what results 8 degrees for $\xi_1 = 0.07$.

In the latest time the temperature box with thermo-electrical elements has been manufactured for rubber beam cooling in the proposed experimental setup. The minimum achieved temperature by the box was -7°C . The identified dynamic Young modulus of the tested rubber is shown in the Fig. 8. It can be predicted from this dependence that the temperature transition zone of this material is cca -20°C up to $+20^\circ\text{C}$. In this zone elastomers undergo crystallization from a fluid to glassy state with substantial increase of stiffness. Since our room fatigue tests were performed in higher temperature out of the zone the rubber was very resistant against a mechanical damage and only small parameter changes were registered.

In the glassy crystallized form there is a very light damping and the elastomers are more receptive to the damage. However the lower temperature were not achievable under the our cooling facility. The data scattering the analytical interpolation curve $E(T)$ in the Fig. 8 can be caused by the material temperature value uncertainty since it was not measured on the beam but in the selected point of the cooling box space.

4. Thermo-mechanical model of kinematic excited beam

a) Swept excitation

For calculation of temperature field of dynamic loaded rubber beam specimen and an estimation of its thermal parameters we came out of the former developed thermo-mechanical finite element model in the COMSOL3.4 environment [7]. Considered material and thermal parameters of the rubber: $\alpha_a = 30 \text{ W/m}^2/\text{°C}$, $\alpha_m = 200 \text{ W/m}^2/\text{°C}$, coefficients of heat transfer into air and steel, respectively, $T_{0a} = T_{0m} = 26 \text{ °C}$ temperatures of air and metal, $\rho = 1357 \text{ kg/m}^3$ density of rubber, $E_0 = 55 \text{ MPa}$ Young modulus, $\mu = 0.49$ Poisson constant, $\beta_K = 2 \times 10^{-3}$ (8% damping ratio) stiffness coefficient of proportional damping.

Temperature T_1 of the beam (see Fig. 3) was measured during the swept loading. The ascertained temperature time characteristic was used to set a specific heat coefficient c_p and a heat transfer coefficient λ . Besides the experimental temperature characteristic the computed characteristics of two variants of these thermal constants are depicted in the Fig. 9: A) $c_p = 500 \text{ J/kg/°C}$, $\lambda = 0.28 \text{ W/m/°C}$; B) $c_p = 800 \text{ J/kg/°C}$, $\lambda = 0.38 \text{ W/m/°C}$. As was proven from the calculations the lower is a coefficient c_p the higher is a maximum temperature and the higher is a coefficient λ the steeper is a temperature increase in the resonance vibration (heating) and the faster is a temperature decrease after the resonance vibration (cooling process).

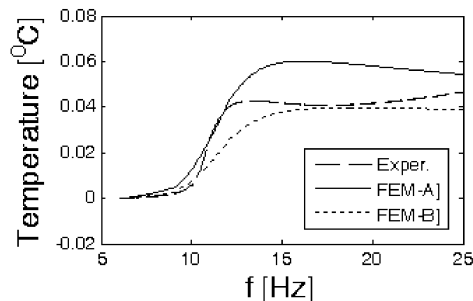


Fig.9: Temperature time characteristics of T_1 obtained experimentally and by numerical simulations for two variants of thermal constants

The excitation of the numerical simulations modeled the experimental swept excitation (see Fig. 4) in a frequency range from 6 Hz up to 25 Hz with a rate 0.1 Hz/s. Due to decomposition of thermo-mechanical coupling to diminish the calculation time the swept excitation was divided into three time blocks with harmonic excitation $y(t) = \ddot{y}_z(t)/(2\pi f(t))^2 \sin(2\pi f(t)t)$ having different amplitudes and frequencies: I) $f_1 = 8 \text{ Hz}$, $y_{b1} = 2 \times 10^{-3}$ for $t \in \langle 0, 30 \rangle \text{ s}$, II) $f_2 = 12.8 \text{ Hz}$, $y_{b2} = 0.7 \times 10^{-3}$ (resonance) for $t \in \langle 30, 60 \rangle \text{ s}$, III) $f_3 = 18 \text{ Hz}$, $y_{b3} = 0.5 \times 10^{-3}$ for $t \in \langle 60, 190 \rangle \text{ s}$.

b) Cyclic excitation

For an estimation of temperature field in the rubber beam at stationary resonance flexural vibration the same FE calculation as described above (variant B) was performed with the harmonic excitation having an amplitude $y_b = 1 \times 10^{-3}$ m and frequency $f = 12.8$ Hz. Contour color plot of temperatures on the beam surface after 1000 s of the resonance vibration due to the thermo-mechanic heating is in the Fig. 10. The temperature T_1 (near the clamping) increase during this loading is shown in the Fig. 11. The computed temperature growth was confirmed by the contactless point temperature measurement by the IR temperature sensor.

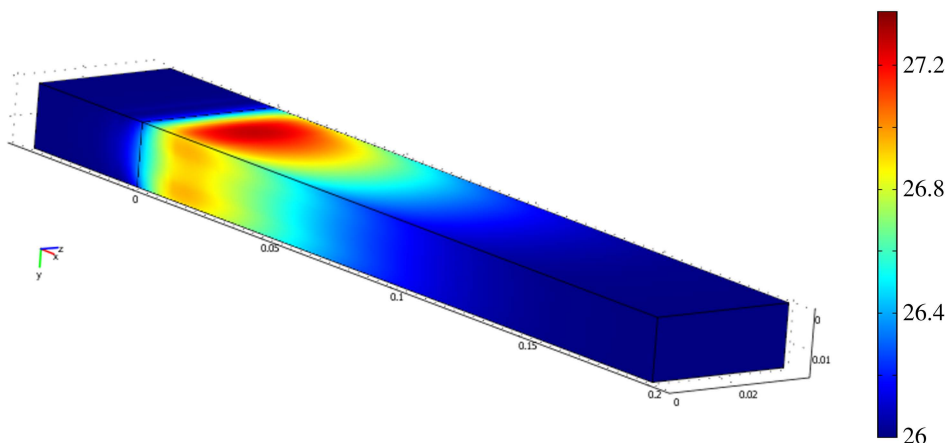


Fig.10: Temperature field of the rubber beam after the 1000 s resonance vibration block

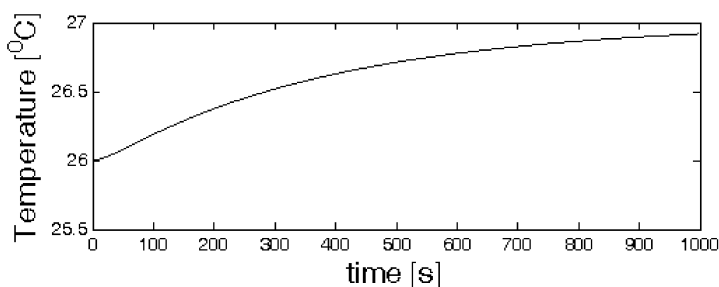


Fig.11: Temperature time characteristic in the point A at the resonance beam vibration

5. Conclusion

In this contribution the new test method for evaluation of thermo-visco-elastic characteristics of elastomers based on the kinematically excited beam under the swept sine excitation is presented. By the swept excitation the first flexural eigenfrequency is crossed over. Mechanic characteristics, i.e. Young modulus and loss angle, are identified from the experimental FRFs by means of the analytical form as developed herein. The experimental

FRF was ascertained both from strain and acceleration responses of the beam and the vibrator table motion. The same results were achieved. For long-term fatigue tests with high level of vibrations the measurement of beam responses by miniature accelerometers seems to be very advantageous. Numerical programs for measured data acquisition, complex FRF evaluation and eigenvalue identification were developed in the environment MATLAB.

The thermal material constants were determined indirectly from the time changeable temperature field and the numerical FE beam model concerning the thermo-mechanic interaction. From an absolute increase of temperature during the harmonic resonant vibration it can be seen very moderate heating of the rubber confirming that the fatigue kinematic rubber tests were negligibly influenced by the temperature effect due to the thermo-mechanic coupling. For the detection of fast and small temperature changes the platinum temperature sensor was manufactured by the thin layer technology.

The short-term tests in the 'sweep' regime serve for an identification of thermal and amplitude material characteristics. The long-term tests with the cyclic loading enable an analysis of material degradation emphasizing a fatigue of material such as hardening effect and arising permanent deformations. The presented results of fatigue tests were achieved at a room temperature. In the next stage the use of thermo-electrical cells will be used for material testing under lower temperatures.

Acknowledgement

This paper has been elaborated in a frame of the grant project GA CR 101/09/1166 Research of dynamic behavior and optimalization of complex rotating systems with non-linear couplings and high damping materials.

References

- [1] Nashif A.D., Johnes D.I.G., Henderson J.P.: Vibration Damping, John Wiley & Sons, 1985
- [2] Schätz M., Vondráček P.: Polymer testing, Institute of Chemical Technology, Prague, 1988, text book (in Czech)
- [3] Pešek L., Půst L., Balda M., Vaněk F., Svoboda J., Procházka P., Marvalová B.: Investigation of dynamics and reliability of rubber segments for resilient wheel, Procs. of ISMA 2008, KU Leuven, 2008, pp.2887–2902
- [4] Daněk O., Kozánek J.: Dynamická analýza nekonzervativních kontinuí, ÚT-ČSAV Praha, učební texty, 1990
- [5] Pešek L.: Global MIMO identification methods in time and frequency domain. Procs. of Eng. Mechanics '99 Conference, Svratka, FME UT Brno, pp.183–188 (in Czech), 1999
- [6] Pešek L., Horáček J., Hendrych P.: Frequency response functions modeling of the human skull with simulation of brain tissue influence, In.: Proc. of Engineering Mechanics 2001, May 14–17, 2001, Svratka, pp. 335–336 (in Czech)
- [7] Pešek L., Šulc P.: FEM 3D Model of Thermal Processes of Vibro-Damping Rubber Elements with Thermo-Mechanical Interaction, Proc. Interaction and Feedbacks 2007, Inst. of Thermo-mechanics AS CR, v.v.i., pp. 43–50, 2007

Received in editor's office: March 18, 2009

Approved for publishing: June 4, 2009

Note: This paper is an extended version of the contribution presented at the national colloquium with international participation *Dynamics of Machines 2009* in Prague.